# Lattice Boltzmann approach for near-field thermal radiation

Yong Chen[1] and Yimin Xuan[1,2,*]

[1]*School of Energy and Power Engineering, Nanjing University of Science and Technology, Nanjing 210094, China*
[2]*School of Energy and Power, Nanjing University of Aeronautics and Astronautics, Nanjing 210016, China*

The lattice Boltzmann (LB) approach is presented for the near-field thermal radiation (including the contributions of the propagating and evanescent waves). The radiative transfer equations in the medium and on the interface are derived for the propagating and evanescent waves from the Maxwell equations, respectively. The Chapman-Enskog analysis is adopted to derive the LB model to recover the radiative transfer equation. The scattering parameter coefficient $\eta$ is proposed to demonstrate the wave behavior of photons on the interface between medium and vacuum. The numerical tests are implemented to solve the near-field radiative heat transfer between two slabs by using the proposed LB approach. The accuracy of the LB model can be improved by increasing the resolution of the wave-number space. By comparing with the benchmark of analytical solutions, the proposed numerical approach enables computing the near-field thermal radiation with good accuracy and exhibits promising applications in dealing with complicated near-field thermal radiation processes.

## I. INTRODUCTION

The radiative heat flux between two objects can exceed the blackbody limit when the distance between the two objects is at the micro- and nanoscales. Numerous studies in the past decades were devoted to exploiting the numerical methods for calculating the near-field radiative heat transfer efficiently [1–4]. In contrast to the traditional far-field thermal radiation, the near-field thermal radiation can break the blackbody limit due to the evanescent waves and the tunneling effects of the photons [3,5]. In order to understand the underlying physical mechanisms of the near-field thermal radiation, several methods were exploited to tackle the problems of near-field thermal radiation based on the Maxwell equations. The dyadic Green's function method has been widely derived to calculate the near-field thermal radiation between two ideal plane slabs [1,2,4]. However, the rigorous analytical solutions were limited to regular geometries such as plane slabs [6,7] and spheres [8,9]. The analytical expressions of the near-field thermal radiation between the complicated geometries cannot be given directly by the dyadic Green's method. Fortunately, the numerical methods can solve the problems of complicated structures by discretizing the computational space. The components of electric and magnetic fields at every grid node can be obtained by the numerical methods and then the radiative energy fluxes can be computed by the Poynting vector. Hence, the numerical method has attracted much attention in the studies of the near-field radiative heat transfer between complicated structures. Wen [10] has proposed the numerical method to calculate the near-field thermal radiation by using the finite-difference time domain (FDTD) method based on the Wiener Chaos expansions. The results agree well with the

Green's function method. Liu [11] has further used the same method to demonstrate the near-field radiative heat transfer between the plane slab and nanowire array and illustrated the physical mechanism of the broadband near-field thermal emitter (absorber) based on the metamaterial of nanowire arrays. Rodriguez *et al.* [12]. have presented the numerical approach on basis of the FDTD method, in which the white noise has been used to model the spontaneous emission. The presented numerical method can deal with arbitrary geometries and materials. Rodriguez *et al.* [13] have further derived a fluctuating-surface-current formulation of radiative heat transfer. Based on the sophisticated numerical techniques of the boundary element method, the exploited formulas can solve the near-field radiative heat transfer between the arbitrary structures efficiently. However, the numerical methods for calculating the near-field radiative heat flux based on the electromagnetic theory have to figure out the intermediate variables (the electric and magnetic fields) at every grid point in order to obtain the Poynting vector (radiative heat flux), leading to that the calculating procedure can cost a great deal of computing resources. Naturally, the calculating procedures can be simplified and accelerated when the numerical method can avoid calculating the intermediate variables and directly iterate the radiative heat transfer. It is intriguing that the particlelike nature of the photon indicates the inherent advantage of the lattice Boltzmann (LB) method for simulating the thermal radiation problems. The LB method, which originates from mesoscopic kinetic equations and has been used to simulate the hydrodynamic systems by modeling the particle migration [14–16], has been extensively investigated to model the energy transport problems by modeling the energy carrier (phonon or electron) migration [17–20]. The LB method can simulate the thermal radiation transfer directly by modeling the transport of the energy carriers (photons) without the intermediate variables. Moreover, the LB method is a promising

---

*Corresponding author: ymxuan@nuaa.edu.cn

　　　　　　　　043308-1

numerical approach for modeling radiative heat transfer due to the fact that the LB method has simple calculation procedures, and high computational performance [21,22].

Numerous works demonstrated the feasibility of the LB method for simulating far-field thermal radiation problems. Ma *et al.* [22] derived the one-dimensional LB method for the radiation transfer based on the radiation hydrodynamics. The macroscopic conservation equations and the radiation momentum are derived. By comparing with the exact solutions of finite-volume method (FVM), it can be concluded that the proposed model in Ref. [22] has good accuracy for solving the one-dimensional radiative heat transfer. Luo *et al.* [23] has developed the discrete unified gas kinetic scheme to model the radiative heat transfer in the participating media based on the Boltzmann equations. Comparing with the conventional numerical models, the present method can give accurate numerical solutions with relative coarse grids and higher computational efficiency. Mchardy *et al.* [24] has demonstrated the LB method for three-dimensional radiation transfer problem and proposed a new iterative algebraic approach for the scattering phase function. By comparing with the solutions provided by Monte Carlo simulations, the study has shown good accuracy of the LB method on modeling the thermal radiation. Yi *et al.* [25] proposed a complete LB model for the steady radiative transfer equation. The D2Q9 model was used to simulate the multidimensional radiative heat transfer problems in order to test the proposed model. The obtained results indicate highly accurate comparing with the other methods or analytical solutions. In addition, the author indicates that the presented LB model is highly adaptable to a multiphysics coupling simulation by applying the model to the coupled radiation and conductive heat transfer problems. However, the LB method for the traditional radiative heat transfer has not been widely used in the coupling computations of radiative and conductive heat transfer. The thermal radiation in the existing coupling calculation has been provided by the FVM [26,27] and discrete ordinate method [28]; meanwhile, the conductive heat transfer has been simulated by LB method. The coupling calculation between two different methods results in the additional difficulty for the simulating procedures. Especially, the near-field radiative heat transfer can exceed the blackbody limit [7,29–31] while the existing methods for the near-field radiative heat transfer are difficult to apply to the coupling simulation.

According to the above descriptions, the investigation of the LB approach for the near-field thermal radiation exhibits great importance for the simulation of the near-field thermal radiation as well as for coupling computation of the radiative and conductive heat transfer. However, the existing LB model cannot be applied to the near-field thermal radiation directly due to that the propagation of the evanescent waves cannot satisfy the radiation hydrodynamics. The LB approach for the near-field thermal radiation should be further derived based on electromagnetic wave intrinsic of thermal radiation.

In this work, we derive the LB approach for the near-field thermal radiation transfer based on the electromagnetic theory. Different from the radiation hydrodynamics, both the traditional and near-field thermal radiation can be solved by the presented numerical model. The detailed theoretical model is illustrated in Sec. II of this article. In Sec. II A, the

detailed derivations of the LB model for the near-field thermal radiation are illustrated based on Maxwell equations. Section II B demonstrates the transmission of the photons at the interface by the scattering theory. The scattering coefficient $\eta$ is proposed to model the wave behavior of the photons on the interface. In Sec. II C, the Chapman-Enskog analysis is used to recover the radiative transfer equation by the proposed LB model. Sections II D and II E illustrate the boundary conditions and computational procedure, respectively. In Sec. III of this paper, the near-field radiative heat transfer between the two smooth slabs is simulated by the presented numerical model for the purpose of validating the proposed LB model. The simulating precession is improved by increasing the resolution of the wave-number space. The simulating results are compared with the benchmark provided by the analytical solutions (dyadic Green's function method), which indicates that the presented LB model can be successfully applied to modeling the near-field radiative heat transfer with good accuracy.

## II. THEORY

### A. The radiative transfer equation based on electromagnetic theory

The radiation hydrodynamic theory fails to illustrate near-field radiative heat transfer because evanescent waves cannot propagate freely in the vacuum. The near-field thermal radiation is intrinsically electromagnetic wave so that it can be demonstrated by the Maxwell equations [32]

$$\nabla \times \mathbf{H}(\mathbf{r}, t) = \varepsilon_0 \varepsilon_r \frac{\partial \mathbf{E}(\mathbf{r}, t)}{\partial t} + \mathbf{J}(\mathbf{r}, t)$$

$$\nabla \times \mathbf{E}(\mathbf{r}, t) = -\mu_0 \mu_r \frac{\partial \mathbf{H}(\mathbf{r}, t)}{\partial t}, \tag{1}$$

where $\mathbf{E} = (E_x, E_y, E_z)$, $\mathbf{H} = (H_x, H_y, H_z)$ are, respectively, electric and magnetic fields. The bold symbols indicate the quantities are vectors. $\mathbf{J} = (J_x, J_y, J_z)$ represents the current source term, $\mathbf{r} = (x, y, z)$ is for the position vector, and $\varepsilon_0$ and $\mu_0$ are, respectively, for the permittivity and permeability in the vacuum while $\varepsilon_r = \varepsilon'_r + i\varepsilon''_r$ and $\mu_r = \mu'_r + i\mu''_r$ are, respectively, for the relative dielectric function and the magnetic permeability of the material. The dielectric function $\varepsilon_r$ and the magnetic permeability $\mu_r$ are the complex numbers. The real part indicates the impedance of the medium and the imaginary part leads to the polarization loss in the medium. $t$ is the symbol of time.

By combining Eq. (1) and the vector identity $\nabla \cdot (\vec{a} \times \vec{b}) = \vec{b} \cdot \nabla \times \vec{a} - \vec{a} \cdot \nabla \times \vec{b}$, the complex Poynting vector can satisfy the following expression:

$$\nabla \cdot (\mathbf{E} \times \mathbf{H}^*) = (i\omega\mu_0\mu_r \mathbf{H} \cdot \mathbf{H}^* - i\omega\varepsilon_0\varepsilon_r^* \mathbf{E} \cdot \mathbf{E}^*) - q, \tag{2}$$

where $q = \mathbf{E} \cdot \mathbf{J}^*$ is the fluctuation-dissipation source term.

In this work, the following derivation is based on the assumption of the isotropic materials. Hence, expression (2) can be expanded as

$$\frac{\partial(E_y H_z^* - E_z H_y^*)}{\partial x} = \frac{1}{2} \begin{pmatrix} i\omega\mu_0\mu_r(H_z H_z^* + H_y H_y^*) \\ -i\omega\varepsilon_0\varepsilon_r(E_z E_z^* + E_y E_y^*) \end{pmatrix} - q_x, \tag{3}$$

$$\frac{\partial(E_z H_x^* - E_x H_z^*)}{\partial y} = \frac{1}{2}\begin{pmatrix} i\omega\mu_0\mu_r(H_z H_z^* + H_x H_x^*) \\ -i\omega\varepsilon_0\varepsilon_r(E_z E_z^* + E_x E_x^*) \end{pmatrix} - q_y,$$

(4)

$$\frac{\partial\left(E_x H_y^* - E_y H_x^*\right)}{\partial z} = \frac{1}{2}\begin{pmatrix} i\omega\mu_0\mu_r(H_x H_x^* + H_y H_y^*) \\ -i\omega\varepsilon_0\varepsilon_r(E_x E_x^* + E_y E_y^*) \end{pmatrix} - q_z.$$

(5)

Here, we deal with expression (5) as an example, which stands for the TM mode radiative heat flux in the $z$ direction. When the radiative heat flux is assumed to be monochromatic, the dielectric function $\varepsilon_r$ and the magnetic permeability $\mu_r$ are regarded as constant. By using the harmonic factor $e^{-i\omega t}$, the monochromatic electric field **E** and magnetic field **H** can be written as the complex form below [32–34]:

$$E_\xi(\mathbf{r}, t) = E_{\xi,0}(x, y)e^{i\gamma' z}e^{-\gamma'' z}e^{-i\omega t},$$

(6)

$$H_\xi(\mathbf{r}, t) = H_{\xi,0}(x, y)e^{i\gamma' z}e^{-\gamma'' z}e^{-i\omega t},$$

(7)

in which, $\xi = x, y, z$ represents the axis directions. $E_0$ and $H_0$ are for the amplitudes of electromagnetic fields. $i$ represents the symbol of imaginary part of complex number. Expression (6) indicates that the electromagnetic field propagates in the direction of axis $z$ with the propagation constant $\gamma = \gamma' + i\gamma''$, where $\gamma$ is a complex number. The propagation constant $\gamma$ satisfies the following expression [32]:

$$\gamma = \sqrt{k^2 - \kappa^2},$$

(8)

where $k = \omega\sqrt{\mu_0\varepsilon_0\mu_r\varepsilon_r}$ is the wave number in the medium. The wave number in vacuum is $k_0 = \omega\sqrt{\mu_0\varepsilon_0}$. $\kappa \geqslant 0$, which is a real number, is the horizontal wave number perpendicular to the axis $z$. The dielectric function $\varepsilon_r$ and the magnetic permeability $\mu_r$ equal 1 if the medium is vacuum. According to expression (8), $\gamma$ is a pure complex in vacuum if $\kappa > k_0$. Expressions (6)–(8) are used in this work based on the assumption that the thermal radiation fluxes are independent for each frequency and wave number. Based on the superposition theorem, the total radiative heat flux can be obtained by integrating the monochromatic radiative heat fluxes over the wave numbers and frequencies.

Considering the case that the monochromatic electromagnetic waves propagate in the direction of axis $z$, the partial derivatives with respect to $t$ and $z$ can be replaced by $\partial/\partial t = -i\omega$ and $\partial/\partial z = i\gamma$. Then, the two source-free curl equations in Eq. (1) can be expanded as following [34]:

$$\frac{\partial H_z}{\partial y} - i\gamma H_y = -i\omega\varepsilon_0\varepsilon_r E_x$$

$$i\gamma H_x - \frac{\partial H_z}{\partial x} = -i\omega\varepsilon_0\varepsilon_r E_y$$

$$\frac{\partial H_y}{\partial x} - \frac{\partial H_x}{\partial y} = -i\omega\varepsilon_0\varepsilon_r E_z,$$

$$\frac{\partial E_z}{\partial y} - i\gamma E_y = i\omega\mu_0\mu_r H_x$$

$$i\gamma E_x - \frac{\partial E_z}{\partial x} = i\omega\mu_0\mu_r H_y$$

$$\frac{\partial E_y}{\partial x} - \frac{\partial E_x}{\partial y} = i\omega\mu_0\mu_r H_z.$$

(9)

(10)

According to expressions (9) and (10), the transverse field components $E_x$, $E_y$ and $H_x$, $H_y$ can be, respectively, expressed in terms of the longitudinal field components $E_z$ and $H_z$, which can be written as [34]

$$H_x = \frac{i}{\kappa^2}\left(\gamma\frac{\partial H_z}{\partial x} - \omega\varepsilon_0\varepsilon_r\frac{\partial E_z}{\partial y}\right),$$

(11)

$$H_y = \frac{i}{\kappa^2}\left(\gamma\frac{\partial H_z}{\partial y} + \omega\varepsilon_0\varepsilon_r\frac{\partial E_z}{\partial x}\right),$$

(12)

$$E_x = \frac{i}{\kappa^2}\left(\gamma\frac{\partial E_z}{\partial x} + \omega\mu_0\mu_r\frac{\partial H_z}{\partial y}\right),$$

(13)

$$E_y = \frac{i}{\kappa^2}\left(\gamma\frac{\partial E_z}{\partial y} - \omega\mu_0\mu_r\frac{\partial H_z}{\partial x}\right).$$

(14)

On the basis of the classic definition, the transverse magnetic (TM) wave and the transverse electric (TE) wave indicate the components of the magnetic field $H_z = 0$ and electric field $E_z = 0$, respectively [34,35]. In this paper, the TM wave is illustrated as an example. The similar procedure can be applied to the derivation for the TE wave. Therefore, the formulas (11)–(14) for the TM mode can be written as

$$H_x = \frac{-i\omega\varepsilon_0\varepsilon_r}{\kappa^2}\frac{\partial E_z}{\partial y},$$

(15)

$$H_y = \frac{i\omega\varepsilon_0\varepsilon_r}{\kappa^2}\frac{\partial E_z}{\partial x},$$

(16)

$$E_x = \frac{i\gamma}{\kappa^2}\frac{\partial E_z}{\partial x},$$

(17)

$$E_y = \frac{i\gamma}{\kappa^2}\frac{\partial E_z}{\partial y}.$$

(18)

The TM mode radiative heat flux $I_{z,TM}$ in the $z$ direction can be figured out by the Poynting vector, which is written as [1]

$$I_{z,TM} = 2\mathrm{Re}[\mathbf{E} \times \mathbf{H}^*]\hat{z} = 2\mathrm{Re}[E_x H_y^* - E_y H_x^*],$$

(19)

where * is the symbol of conjugate and Re[] represents the real part of complex number. $\hat{z}$ is the unit direction vector. Substituting formulas (15)–(18) into (19) gives

$$I_{z,TM} = 2\omega\varepsilon_0\mathrm{Re}[\gamma\varepsilon_r^*]D.$$

(20)

Here, the intermediate variable $D$ is defined as

$$D = \frac{1}{\kappa^4}\left(\left|\frac{\partial E_z}{\partial x}\right|^2 + \left|\frac{\partial E_z}{\partial y}\right|^2\right).$$

(21)

Similarly, substituting formulas (15)–(18) into (5) gives the formula in the $z$ direction

$$\frac{\partial I_{z,TM}}{\partial z} = \begin{pmatrix} i\omega\left(\mu_0\mu'_r\omega^2\varepsilon_0^2|\varepsilon_r|^2 - \varepsilon_0\varepsilon'_r|\gamma|^2\right) \\ -\omega\left(\mu_0\mu''_r\omega^2\varepsilon_0^2|\varepsilon_r|^2 + \varepsilon_0\varepsilon''_r|\gamma|^2\right) \end{pmatrix}D - q_z.$$

(22)

According to expressions (19)–(22), the near-field radiative heat flux can be written as the following:

$$\frac{\partial I_{z,TM}}{\partial z} = -\beta I_{z,TM} - q_z,$$

(23)

in which the extinction coefficient $\beta$ is expressed as the following:

$$\beta = k_0 \left( \frac{\mu''_r |\varepsilon_r|^2 + \varepsilon''_r |\tilde{\gamma}|^2}{2\mathrm{Re}[\tilde{\gamma}\varepsilon_r^*]} \right), \tag{24}$$

where $k_0 = \omega\sqrt{\mu_0\varepsilon_0}$ is the wave number in the vacuum. $\tilde{\gamma} = \gamma/k_0$ is dimensionless propagation constant.

By employing the same processes as (9)–(24), the radiative heat flux in the $x$ and $y$ direction can result in the similar expressions

$$\frac{\partial I_{x,TM}}{\partial x} = -\beta I_{x,TM} - q_x, \tag{25}$$

$$\frac{\partial I_{y,TM}}{\partial y} = -\beta I_{y,TM} - q_y, \tag{26}$$

where the parameter $\beta$ is the same as that in expression (23) because the derivation is based on the homogeneous material.

The source term $q$ in the isotropic materials can be obtained by the fluctuation-dissipation theory [3]

$$\langle \vec{J}_n(\vec{r}', \omega)\vec{J}_m^*(\vec{r}'', \omega') \rangle$$
$$= \frac{\omega\varepsilon_0\varepsilon''}{\pi}\Theta(\omega, T)\delta(\vec{r}' - \vec{r}'')\delta(\omega - \omega')\delta_{nm}, \tag{27}$$

where $\langle\rangle$ is the symbol of ensemble average. $\Theta(\omega, T)$ is the average energy of Planck's oscillator, $T$ is temperature of the grid point, $\omega$ is the frequency. $\delta(\vec{r}' - \vec{r}'')$ and $\delta(\omega - \omega')$ are Dirac function. $\delta_{nm}$ is the Kronecker function, which satisfies the expressions $\delta_{nm} = 1(n = m)$ and $\delta_{nm} = 0(n \neq m)$. $n$ and $m$ are the polar direction of the fluctuating current. $\delta_{nm}$ indicates the assumption of isotropic material [1].

The polar current in the material satisfies the relation of $\mathbf{J} = \omega\varepsilon_0\varepsilon''_r\mathbf{E}$ [34], and then the source term in formula (2) can be expressed as the following:

$$q = \frac{\mathbf{J} \cdot \mathbf{J}^*}{\omega\varepsilon_0\varepsilon''_r}. \tag{28}$$

Combining expression (27) with (28), the source term can be further written as

$$q = \frac{\Theta(\omega, T)\delta(\mathbf{r}' - \mathbf{r}'')\delta(\omega - \omega')\delta_{mn}}{\pi}. \tag{29}$$

So far we have obtained the radiative transfer equation of the equilibrium state in the isotropic materials on basis of the electromagnetic theory. The superposition of the radiative heat fluxes in Eqs. (23), (25), and (26) can obtain the common formulation in any direction and is expressed as follows:

$$\nabla \cdot (\hat{s}I_{s,TM}) = -\beta I_{s,TM} - q, \tag{30}$$

where $\hat{s}$ indicates the unit vector in the propagating direction. Similarly, the expressions for the TE mode radiative heat transfer are illustrated in Appendix A by using the same procedure.

The total near-field radiative heat transfer can be obtained by integrating the spectral radiative intensity of the TM and TE waves over the frequency domain and wave-vector domain, which can be expressed as

$$P(\mathbf{r}) = \int_\omega \int_\kappa [I_{TM}(\omega, \kappa, \mathbf{r}) + I_{TE}(\omega, \kappa, \mathbf{r})]d\kappa d\omega, \tag{31}$$
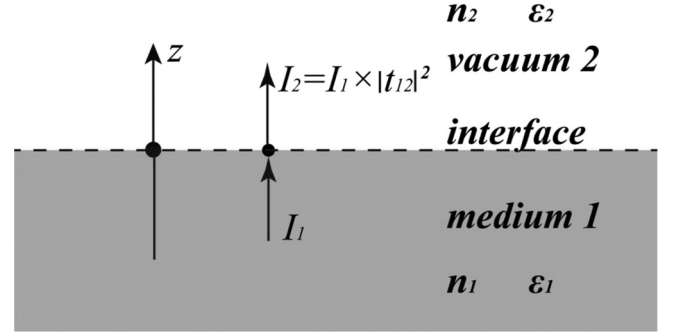


FIG. 1. Schematic profile of the interface between medium and vacuum.

where $P(\mathbf{r})$ is the net near-field radiative heat flux at the position $\mathbf{r}$.

The radiative transfer equation (30) is derived based on the Maxwell equations, which indicates that the near-field thermal radiation can also be demonstrated by the derived radiative transfer equation. Nevertheless, when the evanescent wave ($\kappa > k_0$) [3] of the near-field thermal radiation penetrates the interface from the material to vacuum, the incident wave vector $\gamma = \sqrt{k_0^2 - \kappa^2}$ is a pure complex. Hence, the term $\mathrm{Re}[\varepsilon_r^*\tilde{\gamma}]$ is 0 due to $\varepsilon_r^* = 1$ in vacuum, which leads to that the extinction coefficient $\beta$ is approaching infinity. Consequently, it is necessary to further explore the radiative transfer equation for the evanescent waves.

### B. The radiative transfer equation on the interface

The transmission of the incident radiative heat flux can be calculated by the scattering theory [1,3,36]. As is plotted in Fig. 1, the radiative heat flux is transferred from material 1 to vacuum 2. According to Eq. (20), the TM mode radiative heat flux in medium 1 can be written as

$$I_{1,TM} = 2\omega\varepsilon_0\mathrm{Re}[\varepsilon_r^*\gamma]_1 D_1. \tag{32}$$

According to the scattering theory, the horizontal wave number of the electromagnetic field must satisfy the matching condition, which indicates that $\kappa_1$ and $\kappa_2$ are equal. The radiative heat flux transmitting from material 1 to vacuum 2 can be written as

$$I_{2,TM} = 2\omega\varepsilon_0\mathrm{Re}[\varepsilon_r^*\gamma]_1 D_1|t_{12}|^2, \tag{33}$$

where the subscripts 1 and 2 indicate the medium and vacuum, respectively. The $t_{12}$ is the field-transmission coefficient from medium 1 to 2 for the TM wave [36]. By using the following expression in Ref. [36],

$$\mathrm{Re}[\varepsilon_r^*\gamma]_1|t_{12}|^2 = \frac{|n_1|^2|\gamma_1|^2}{|n_2|^2|\gamma_2|^2}\begin{pmatrix}\mathrm{Re}(\varepsilon_r^*\gamma)_2(1 - |r_{12}|^2)\\ -2\mathrm{Im}(\varepsilon_r^*\gamma)_2\mathrm{Im}(r_{12})\end{pmatrix}. \tag{34}$$

Then the propagating wave ($p$ wave) and evanescent wave ($e$ wave) in vacuum can be, respectively, written as

$$I_{2,TM} = \begin{cases} 2\omega\varepsilon_0\mathrm{Re}[\varepsilon_r^*\gamma]_2 D_1(1 - |r_{12}|^2)\frac{|n_1|^2|\gamma_1|^2}{|n_2|^2|\gamma_2|^2} & p \text{ wave} \\ 2\omega\varepsilon_0\mathrm{Im}[\varepsilon_r^*\gamma]_2 D_1(-2\mathrm{Im}[r_{12}])\frac{|n_1|^2|\gamma_1|^2}{|n_2|^2|\gamma_2|^2} & e \text{ wave} \end{cases}, \tag{35}$$

where $n = \sqrt{\varepsilon_r \mu_r}$ are the complex refractive index of the materials. $r_{12}$ is the field reflection coefficient of the TM mode wave. The reflection coefficient $r_{12}$ can be obtained by the scattering theory [4]. The symbol Im[] is for the imaginary part of the complex variable.

From the formulas in (35) and Eq. (30), the radiative transfer equation for the near-field thermal radiation can be written as

$$\hat{s} \cdot \nabla I_{TM} = -\beta I_{TM} - q \qquad (36)$$

where $\beta$ has different form for the $p$ wave and $e$ wave that are given as

$$\beta = \begin{cases} k_0 \left( \frac{\mu''_r |\varepsilon_r|^2 + \varepsilon''_r |\tilde{\gamma}|^2}{2\mathrm{Re}[\tilde{\gamma}\varepsilon_r^*]} \right) & p \text{ wave} \\ k_0 \left( \frac{\mu''_r |\varepsilon_r|^2 + \varepsilon''_r |\tilde{\gamma}|^2}{2\mathrm{Im}[\tilde{\gamma}\varepsilon_r^*]} \right) & e \text{ wave} \end{cases}. \qquad (37)$$

By employing the same derivation procedure as that of the TM mode waves, the expressions of the TE mode radiative transfer equation for the near-field thermal radiation are similarly obtained (illustrated in Appendix B).

### C. The lattice Boltzmann model for near-field thermal radiation

The steady-state near-field radiative heat transfer equation has been derived based on electromagnetic theory. The time variation term and scattering parameter are added to Eq. (36) in order to obtain the Eulerian conservation equation [22]. Thus, we have the following equation:

$$\frac{\partial I}{v \partial t} + \hat{s} \cdot \nabla I = -\beta \eta I - q, \qquad (38)$$

where $v$ is the light speed. The coefficient $\eta$ represents the weight of scattering effects.

The general form of evaluation equation of the LB model yields [22]

$$f_s(\mathbf{r} + \vec{v}_s \Delta t, t + \Delta t) - f_s(\mathbf{r}, t)$$
$$= -\frac{1}{\tau_s} \big[ f_s(\mathbf{r}, t) - f_s^{eq}(\mathbf{r}, t) \big] + \Delta t Q_s(\mathbf{r}, t), \qquad (39)$$

where $\tau_s$ is the dimensionless relaxation time. $\vec{v}_s = \Delta \mathbf{r} / \Delta t$ is the discrete velocity in the direction $s$. $\Delta t$ is the time step in the simulation. $Q_s$ represents the source term. $f_s(\mathbf{r}, t)$ is the distribution function of the particle and $f_s^{eq}(\mathbf{r}, t)$ is the distribution function in the equilibrium state. By using the carefully defined grid models and the proper distribution functions, the near-field radiative transfer equation (38) can be evaluated by the corresponding LB model in Eq. (39).

Without loss of generality, the LB model is applied to solve the near-field thermal radiation between two plane slabs and the D1Q2 model is adopted, which is depicted in Fig. 2. The equilibrium state of the distribution function is artificially defined as the following:

$$f_s^{eq} = \delta_s I_s / v_s, \qquad (40)$$

where $I_s$ the scalar value of the radiative heat flux $\vec{I}_s$ is the $s$ direction. $v_s$ is the velocity of the light. $\delta_s$ is defined as

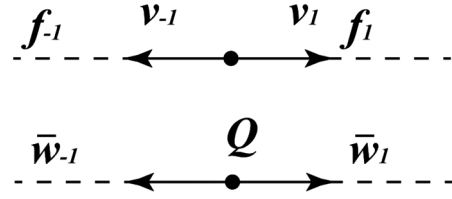$$\delta_s = \begin{cases} 1 & s = 1 \\ -1 & s = -1 \end{cases}. \qquad (41)$$



FIG. 2. Schematic profile of the D1Q2 lattice model in the proposed LB approach.

From the definition of expressions (40) and (41), we can conclude that the equilibrium distribution is related to the scalar value of the radiative heat flux $\vec{I}_s$. The source term satisfies the following expressions:

$$Q_s = \bar{w}_s Q, \qquad (42)$$

$$\bar{w}_{-1} = \bar{w}_1 = \tfrac{1}{2}, \qquad (43)$$

where the minus sign (–) indicates the negative direction. $\bar{w}_{-1,1}$ is the weight of the source term.

First, the Chapman-Enskog analysis is performed to recover the radiative transfer equation from the LB model in Eq. (39). The time and space derivatives are given,

$$\nabla = \varepsilon \nabla_1, \qquad (44)$$

$$\partial_t = \varepsilon \partial_{t1}. \qquad (45)$$

The expanding distribution function and source term can be written as

$$f_s = f_s^{(0)} + \varepsilon f_s^{(1)}, \qquad (46)$$

$$Q_s = \varepsilon Q_s^{(1)}, \qquad (47)$$

where $\varepsilon$ is a small expansion parameter.

By applying Taylor expansion to the term $f_s(\mathbf{r} + \vec{v}_s \Delta t, t + \Delta t)$ in Eq. (39), we can obtain

$$f_s(\mathbf{r} + \vec{v}_s \Delta t, t + \Delta t)$$
$$= f_s(\mathbf{r}, t) + \Delta t (\partial_t + \vec{v}_s \cdot \nabla) f_s(\mathbf{r}, t) + O(\Delta t^2), \qquad (48)$$

$$\Delta t (\partial_t + \vec{v}_s \cdot \nabla) f_s(\mathbf{r}, t)$$
$$= -\frac{1}{\tau_s} \big[ f_s(\mathbf{r}, t) - f_s^{eq}(\mathbf{r}, t) \big] + \Delta t Q_s(\mathbf{r}, t) + O(\Delta t^2). \qquad (49)$$

Combining Eqs. (44)–(47) into Eq. (49), we have

$$(\varepsilon \partial_{t1} + \vec{v}_s \cdot \varepsilon \nabla_1)\big( f_s^{(0)} + \varepsilon f_s^{(1)} \big)$$
$$= -\frac{1}{\Delta t \tau_s} \big[ f_s^{(0)} + \varepsilon f_s^{(1)} - f_s^{eq} \big] + \varepsilon Q_s^{(1)}. \qquad (50)$$

Thus, Eq. (50) can be further written as

$$\big( \varepsilon \partial_{t1} f_s^{(0)} + \vec{v}_s \cdot \varepsilon \nabla_1 f_s^{(0)} \big) + \big( \varepsilon^2 \partial_{t1} f_s^{(1)} + \vec{v}_s \cdot \varepsilon^2 \nabla_1 f_s^{(1)} \big)$$
$$= -\frac{1}{\Delta t \tau_s} \big[ f_s^{(0)} - f_s^{eq} \big] - \frac{1}{\Delta t \tau_s} \varepsilon f_s^{(1)} + \varepsilon Q_s^{(1)}. \qquad (51)$$

By using the scale analysis, the equation in $\varepsilon^0$, $\varepsilon^1$, and $\varepsilon^2$ can be obtained and written as

$$f_s^{(0)} = f_s^{eq}, \tag{52}$$

$$\left(\partial_{t1} f_s^{(0)} + \vec{v}_s \cdot \nabla_1 f_s^{(0)}\right) = -\frac{1}{\Delta t \tau_s} f_s^{(1)} + Q_s^{(1)}, \tag{53}$$

$$\partial_{t1} f_s^{(1)} + \vec{v}_s \cdot \nabla_1 f_s^{(1)} = 0. \tag{54}$$

From Eqs. (40)–(43), we obtain

$$\sum_s v_s f_s^{eq} = \sum_s \delta_s I_s = I, \tag{55}$$

$$\sum_s \vec{v}_s f_s^{eq} = I\hat{s}, \tag{56}$$

$$\sum_s Q_s^{(1)} = Q. \tag{57}$$

According to Eqs. (52)–(54), it yields

$$(\partial_{t1} + \vec{v}_s \cdot \nabla_1) f_s^{eq} = Q_s^{(1)}. \tag{58}$$

By summing Eq. (58) over the direction $s$, the equation can be further written as

$$(\partial_{t1} + \vec{v}_s \cdot \nabla_1) \sum_s f_s^{eq} = \sum_s Q_s^{(1)}. \tag{59}$$

Further substituting expressions (55) and (56) into Eq. (59), we can obtain

$$\frac{\partial I}{v \partial t} + \hat{s} \cdot \nabla_1 I = Q. \tag{60}$$

In order to recover the radiative conservation Eq. (38), we let

$$Q = -\beta \eta I - q \tag{61}$$

Therefore, the LB model can be used to solve the near-field radiative heat transfer problem. The positive coefficient $\eta$ is an important parameter. In the homogeneous medium, $\eta$ is defined as

$$\eta = 1 \quad p/e \text{ wave} \tag{62}$$

However, on the interface between material 1 and vacuum 2, the thermal radiation flux is scattered. $\eta$ can be expressed by the scattering theory according to the formulas (32)–(35)

$$1 - \beta \eta v \Delta t = (1 - |r_{12}|^2) \frac{|n_1|^2 |\gamma_1|^2}{|n_2|^2 |\gamma_2|^2} \quad p \text{ wave}, \tag{63}$$

$$1 - \beta \eta v \Delta t = 2\text{Im}[r_{12}] \frac{|n_1|^2 |\gamma_1|^2}{|n_2|^2 |\gamma_2|^2} \quad e \text{ wave}. \tag{64}$$

### D. Nonreflecting boundary condition

In this paper, nonreflecting boundary conditions are employed to model the free space in vacuum. The absorbing boundary condition for LB method has been presented in Ref. [37] based on the perfect match layer (PML) concept. The PML formulation for three-dimensional linear hyperbolic

systems can be expressed as [37]

$$\frac{\partial \mathbf{U}_x}{\partial t} + \sigma_x \mathbf{U}_x + \mathbf{A}_x \frac{\partial \mathbf{U}}{\partial x} = 0, \tag{65}$$

$$\frac{\partial \mathbf{U}_y}{\partial t} + \sigma_y \mathbf{U}_y + \mathbf{A}_y \frac{\partial \mathbf{U}}{\partial y} = 0, \tag{66}$$

$$\frac{\partial \mathbf{U}_z}{\partial t} + \sigma_z \mathbf{U}_z + \mathbf{A}_z \frac{\partial \mathbf{U}}{\partial z} = 0, \tag{67}$$

where $\mathbf{U}$ is the 3 vector of unknowns ($\mathbf{U} = \mathbf{U}_x + \mathbf{U}_y + \mathbf{U}_z$), $\mathbf{A}_x$, $\mathbf{A}_y$, and $\mathbf{A}_z$ are the coefficients, respectively. $\sigma_x$, $\sigma_y$, and $\sigma_z$ are the positive damping factors. Then, the equation for the absorbing boundary condition can be obtained by the auxiliary variables [37]

$$\begin{aligned}
\frac{\partial \mathbf{U}}{\partial t} &+ \mathbf{A}_x \frac{\partial \mathbf{U}}{\partial x} + \mathbf{A}_y \frac{\partial \mathbf{U}}{\partial y} + \mathbf{A}_z \frac{\partial \mathbf{U}}{\partial z} \\
&= -(\sigma_x + \sigma_y + \sigma_z)\mathbf{U} - (\sigma_x \sigma_y + \sigma_x \sigma_z + \sigma_y \sigma_z)\mathbf{W}_1 \\
&\quad - \sigma_x \sigma_y \sigma_z \mathbf{W}_2 - \mathbf{A}_x \frac{\partial}{\partial x}[(\sigma_y + \sigma_z)\mathbf{W}_1 + \sigma_y \sigma_z \mathbf{W}_2] \\
&\quad - \mathbf{A}_y \frac{\partial}{\partial y}[(\sigma_x + \sigma_z)\mathbf{W}_1 + \sigma_x \sigma_z \mathbf{W}_2] \\
&\quad - \mathbf{A}_z \frac{\partial}{\partial z}[(\sigma_x + \sigma_y)\mathbf{W}_1 + \sigma_x \sigma_y \mathbf{W}_2],
\end{aligned} \tag{68}$$

where

$$\frac{\partial \mathbf{W}_1}{\partial t} = \mathbf{U} \tag{69}$$

and

$$\frac{\partial \mathbf{W}_2}{\partial t} = \mathbf{W}_1. \tag{70}$$

The absorbing boundary condition for the lattice Boltzmann equation is written as follows:

$$\frac{\partial f_s}{\partial t} + v_x \frac{\partial f_s}{\partial x} + v_y \frac{\partial f_s}{\partial y} + v_z \frac{\partial f_s}{\partial z} = -\frac{f_s - f_s^{eq}}{\tau_s} - \sigma_{PML} \tag{71}$$

where $\sigma_{PML}$ is the positive damping coefficient of the absorbing boundary. By combing Eq. (68) and Eq. (71), $\sigma_{PML}$ equals to the right side of Eq. (68).

### E. Simulating procedure of the proposed lattice Boltzmann model

The LBM for the near-field thermal radiation can be implemented by the following steps:

(1) Initialize the computation zone, set the boundary condition, and confirm the initial conditions (frequency, wave vector, and temperature).

(2) Mesh the space of computation, and confirm the initial condition of each node. Add thermal radiation source to the lossy medium.

(3) Compute the radiative heat flux according to the Eq. (39) until process reaches the stop criterion (the relative error $err = |(I_{t+\Delta t} - I_t)/I_t|$ is small enough).

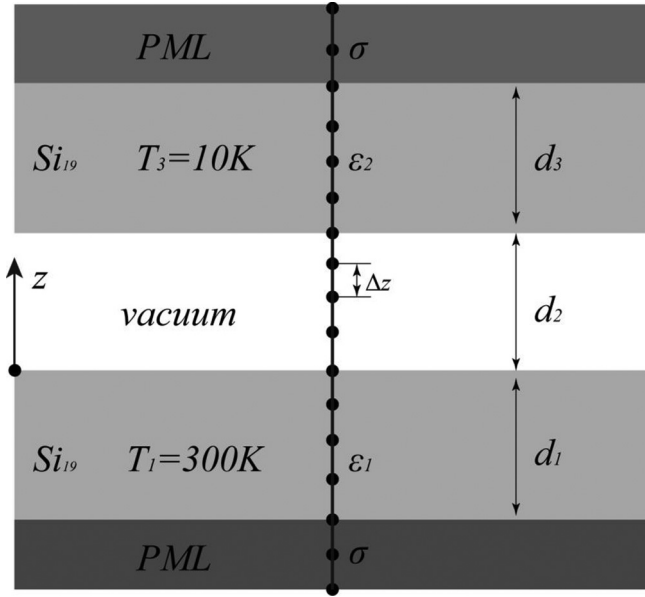(4) Repeat the step 1–3 for another frequency and wave number.

FIG. 3. Schematic sketch of the structure in the numerical simulation.

(5) Terminate the computational process, and integrate the spectral radiative heat flux over the frequencies and wave vectors in order to obtain the total radiative heat transfer.

## III. RESULTS AND DISCUSSION

As an example of the above-mentioned approach, the radiative heat transfer between two parallel semi-infinite slabs is computed to test the proposed LB approach for the near-field thermal radiation in this section. The schematic profile of the plane slabs is depicted in Fig. 3, in which the schematic sketch of the one-dimensional grid is also illustrated. The distance between the slabs is $d_2 = 200$ nm and the temperatures of the slabs are $T_1 = 300$ K and $T_3 = 10$ K, respectively. In the calculations, the material of slabs is doped silicon (the doping concentration of $10^{19}$ cm$^{-3}$). The dielectric function of the doped silicon slabs can be illustrated by the Drude model

$$\varepsilon_r = \varepsilon_\infty - \frac{\omega_p^2}{\omega^2 + i\omega\gamma_p}, \tag{72}$$

where $\varepsilon_\infty = 11.7$ is a high-frequency constant, $\omega_p = 3.42 \times 10^{14}$ rad/s is plasma frequency, and $\gamma_p = 6.12 \times 10^{13}$ rad/s is the scattering rate.

The analytical solution for the near-field thermal radiative heat transfer between two semi-infinite slabs can be given [1,3]

$$P = \frac{1}{4\pi^2} \int_0^\infty [\Theta(\omega, T_1) - \Theta(\omega, T_3)] d\omega \int_0^\infty S(\omega, \kappa)\kappa \, d\kappa, \tag{73}$$

in which the transmission factor $S(\omega,\kappa)$ has different formulations for the propagating wave ($\kappa < \omega/v$, in which $v$ is light

speed in the vacuum) and evanescent wave ($\kappa > \omega/v$). The transmission factor $S(\omega,\kappa)$ is expressed as

$$S_{\text{prop}}(\omega, \kappa) = \sum_{pol=TE,TM} \frac{\left(1 - \left|r_{10}^{\text{pol}}\right|^2\right)\left(1 - \left|r_{20}^{\text{pol}}\right|^2\right)}{\left|1 - r_{10}^{\text{pol}} r_{20}^{\text{pol}} e^{2i\gamma d_0}\right|^2} \kappa < \omega/v, \tag{74}$$

$$S_{\text{evan}}(\omega, \kappa) = \sum_{pol=TE,TM} \frac{4\text{Im}\left[r_{10}^{\text{pol}}\right]\text{Im}\left[r_{20}^{\text{pol}}\right]}{\left|1 - r_{10}^{\text{pol}} r_{20}^{\text{pol}} e^{2\gamma'' d_0}\right|^2} e^{-2\gamma'' d_0} \kappa > \omega/v, \tag{75}$$

where $r$ is the reflective coefficient calculated by scattering theory [3].

The analytical solutions given by expressions (73)–(75) are used as the benchmarks for the purpose of examining the presented LB model. In the calculations the one-dimensional uniform grid has been used. Considering the fact that the near-field thermal radiation transfer occurs in the subwavelength scale (the characteristic length of the structure is smaller than the wavelength), the distance between two neighboring grid points is set at $\Delta z = 10$ nm and the resulting time interval is $\Delta t = \Delta z/v$. The relaxation time $\tau$ can is chosen as $\tau = 0.5$ [22]. The frequency domain in the simulation is set at $2.5 \times 10^{13} \sim 2.0 \times 10^{14}$ rad/s, which covers the dominated wave band of the near-field thermal radiation. The frequency interval is $N_{\text{freq}} = 120$. The computation of the $\kappa$ space is composed of two parts in order to distinguish the propagating ($0 < \kappa < \omega/v$) and evanescent waves ($\pi/\Delta z > \kappa > \omega/v$). The numbers of discrete values of the wave-number space are $N_{\kappa,p} = 100$ and $N_{\kappa,e} = 500$, respectively. The PML boundary is added to the boundary of the structure as is shown in Fig. 3 with the one-dimensional PML for LB model, which is written as

$$\frac{\partial f}{\partial t} + v_z \frac{\partial f}{\partial z} = -\sigma_z. \tag{76}$$

PML thickness is $20\Delta z$ and the damping factor can be defined as $0 < \sigma_z \Delta t < 1$.

According to the resulting curves in Figs. 4(a)–4(b), the TM mode near-field radiative heat transfer modeled by the LB approach coincides with that calculated by analytical solutions. The total radiative heat transfer between the slabs can be obtained by integrating the spectral radiative heat flux over the frequency. According to the integral results in Table I, the relative errors between analytical solution and the results of the LB method are 0.17 and 4.31%, respectively. It can be seen that the proposed lattice Boltzmann model agrees well with the exact solutions. The curves in Figs. 4(c)–4(d) are used to compare the TE mode spectral radiative heat transfer between the plane slabs, which indicates that the numerical results coincide with the analytical solutions. The integrals of the TE mode spectral radiative heat flux are listed in Table I. The absolute difference of the radiative heat transfer between analytical solutions and the numerical models for the TM mode waves is larger than that for TE mode waves. However, the near-field radiative heat transfer between two doped silicon slabs are dominated by the TM mode waves, leading to that the relative errors for the TM mode waves are smaller than that of the TE mode waves.
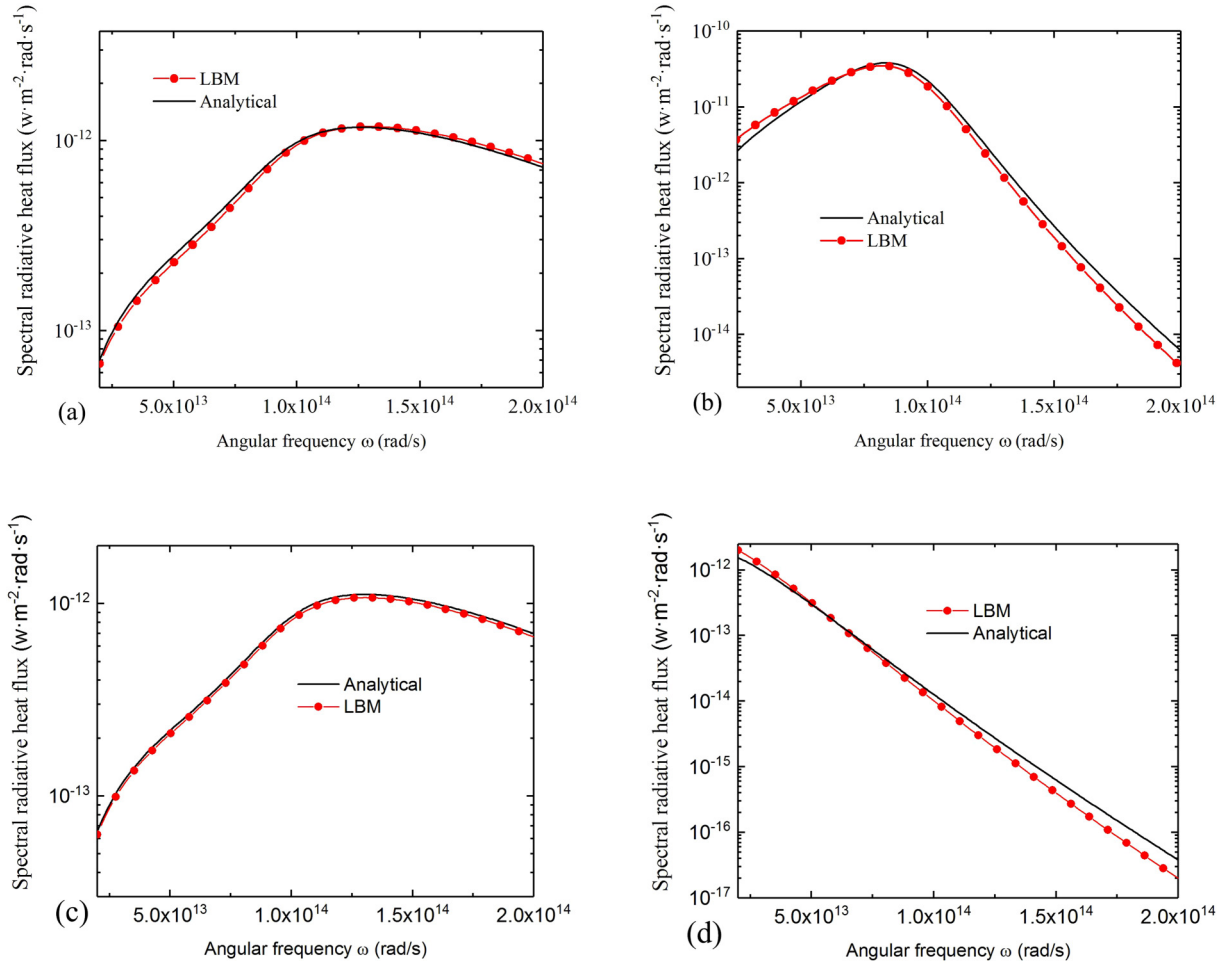
FIG. 4. (a) TM mode propagating wave of the near-field thermal radiation. (b) TM mode evanescent wave of the near-field thermal radiation. (c) TE mode propagating wave of the near-field thermal radiation. (d) TE mode evanescent wave of the near-field thermal radiation.

Further inquiry of the results in Figs. 4(a)–4(d) indicates that the curves deviate from the benchmark curves resulting from the analytical solution in the low-frequency and high-frequency domain. The error trend of the spectral radiative heat flux exhibits similar behavior. Considering that the TM mode waves dominate the near-field radiative heat transfer and the relative errors for the evanescent waves are much larger than that for propagating waves, the near-field radiative heat transfer induced by the TM evanescent waves are therefore further simulated. The intervals of wave-number space are, respectively, further increased to $N_{\kappa,e} = 600$, 800, and 1000 in the simulations. The resulted spectral near-field thermal radiative heat flux is given in Fig. 5. As is depicted in the figure,

the accuracy is apparently improved by increasing the resolutions of the wave-number space. By integrating the spectral near-field thermal radiative heat flux of the case $N_{\kappa,e} = 1000$

TABLE I. The integral results of the radiative heat transfer (unit w/m$^2$).

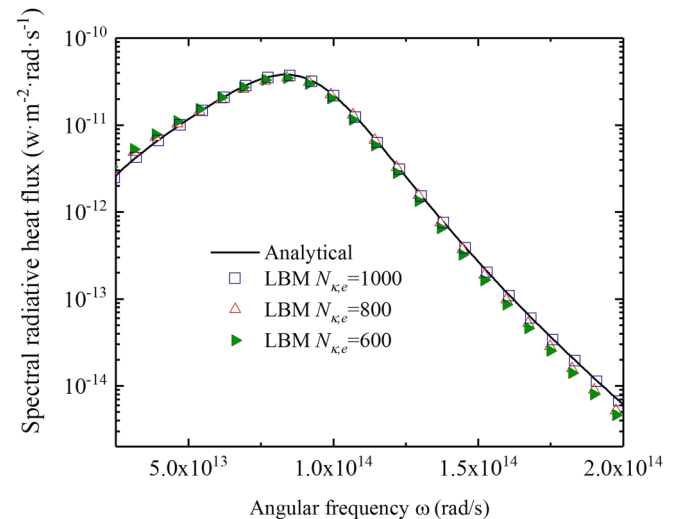|  | Analytical solution | LB method | Relative error |
|---|---|---|---|
| TM $p$ wave | 134.14 | 133.91 | 0.17% |
| TM $e$ wave | 1827.34 | 1748.65 | 4.31% |
| TE $p$ wave | 124.67 | 119.95 | 3.78% |
| TE $e$ wave | 32.39 | 30.77 | 5.00% |



FIG. 5. The results of the TM mode evanescent waves by using the refined resolutions for the wave-number space in the simulations.

over the angular frequency, the resulting near-field thermal radiative heat flux is 1791.51 w/m$^2$ with the relative error reduced to 1.96%, which indicates that the refined resolutions of the wave-number space in the simulations can be adopted to promote the precision of the proposed LB model for near-field thermal radiation.

It is emphasized that for the sake of simplicity and lucidity, here an example of near-field thermal radiation between two adjacent plane surfaces is introduced to show the process how the LB method is applied to handle near-field thermal radiation problems. For multidimensional processes, the main principles and procedures remain similar, but the concrete numerical expressions corresponding to the given problem should be derived and computed.

## IV. CONCLUSIONS

In summary, the LB approach, which has seldom been applied to the near-field thermal radiative heat transfer, is presented for the near-field thermal radiation in this work. The radiative transfer equation for the near-field thermal radiation has been derived on basis of the Maxwell equations. By using the scattering theory, the radiative heat transfer (propagating mode and evanescent mode) on the interface between medium and vacuum is modeled by adding the scattering coefficient $\eta$ to the LB model. Further, the radiative transfer equation for the near-field thermal radiation is derived to be recovered by the LB model. The near-field radiative heat transfer between two semi-infinite plane slabs has been simulated to examining the accuracy of the proposed LB model in this paper. The accuracy of the result is improved by increasing the resolution of the wave-number space. By comparing with analytical solutions, the presented LB model can simulate the near-field thermal radiation with good accuracy. Hence, this work has promising applications in the future for the near-field radiative heat transfer in the nanoscale.

## APPENDIX A: THE RADIATIVE TRANSFER EQUATION FOR THE TE MODE WAVE

For the case of the TE mode waves, the longitudinal electric field $E_z$ is 0, the formulas (11)–(14) can then be written as the following:

$$H_x = \frac{i\gamma}{\kappa^2}\frac{\partial H_z}{\partial x}, \tag{A1}$$

$$H_y = \frac{i\gamma}{\kappa^2}\frac{\partial H_z}{\partial y}, \tag{A2}$$

$$E_x = \frac{i\omega\mu_0\mu_r}{\kappa^2}\frac{\partial H_z}{\partial y}, \tag{A3}$$

$$E_y = \frac{-i\omega\mu_0\mu_r}{\kappa^2}\frac{\partial H_z}{\partial x}. \tag{A4}$$

The TE mode radiative heat flux $I_{TE}$ in the $z$ direction can be figured out by the Poynting vector, which is written as [1]

$$I_{TE}\hat{z} = 2\text{Re}[\mathbf{E}\times\mathbf{H}^*]\hat{z} = 2\text{Re}[E_xH_y^* - E_yH_x^*]\hat{z}, \tag{A5}$$

where * is the symbol of conjugate. $\hat{z}$ is the unit direction vector. The subscript *TE* indicates the TE mode near-field radiative heat flux. Substituting formulas (A1)–(A4) into (A5) gives

$$I_{TE} = 2\omega\mu_0\text{Re}[\mu_r\gamma^*]D_{TE}, \tag{A6}$$

where the intermediate variable is defined as

$$D_{TE} = \frac{1}{\kappa^4}\left(\left|\frac{\partial H_z}{\partial y}\right|^2 + \left|\frac{\partial H_z}{\partial x}\right|^2\right). \tag{A7}$$

Substituting the formulas (A1)–(A4) into Eq. (2), TE mode radiative transfer equation can be obtained by employing the same procedure as that for the TM mode waves; the radiative transfer equation for the TE mode can be written as

$$\hat{s}\cdot\nabla I_{TE} = -\beta_{TE}I_{TE} - q, \tag{A8}$$

in which the extinction coefficient $\beta_{TE}$ is expressed as the following:

$$\beta_{TE} = k_0\frac{(\mu''_r|\tilde{\gamma}|^2 + \varepsilon''_r|\mu_r|^2)}{2\text{Re}[\mu_r\tilde{\gamma}^*]}. \tag{A9}$$

## APPENDIX B: THE RADIATIVE TRANSFER EQUATION ON THE INTERFACE FOR THE TE MODE WAVE

The propagating wave (*p* wave) and evanescent wave (*e* wave) in vacuum can be, respectively, written as

$$I_{2,TE} = \begin{cases} 2\omega\mu_0\text{Re}[\mu_r\gamma^*]_2D_1(1 - |r_{12,TE}|^2)\frac{|n_1|^2|\gamma_1|^2}{|n_2|^2|\gamma_2|^2} & p\text{ wave} \\ 2\omega\mu_0\text{Im}[\mu_r\gamma^*]_2D_1(-2\text{Im}[r_{12,TE}])\frac{|n_1|^2|\gamma_1|^2}{|n_2|^2|\gamma_2|^2} & e\text{ wave} \end{cases}, \tag{B1}$$

where $n_1$ and $n_2$ are the complex refractive index of the materials. $r_{12,TE}$ is the field-reflection coefficient of the TE mode wave.

The radiative transfer equation for the TE mode near-field thermal radiation in any direction can be written as

$$\hat{s}\cdot\nabla I_{TE} = -\beta_{TE}I_{TE} - q, \tag{B2}$$

where the *p*-wave and *e*-wave form of $\beta_{TE}$ are expressed as

$$\beta_{TE} = \begin{cases} k_0\left(\frac{\mu''_r|\tilde{\gamma}|^2 + \varepsilon''_r|\mu_r|^2}{2\text{Re}[\mu_r\tilde{\gamma}^*]}\right) & p\text{ wave} \\ k_0\left(\frac{\mu''_r|\tilde{\gamma}|^2 + \varepsilon''_r|\mu_r|^2}{2\text{Im}[\mu_r\tilde{\gamma}^*]}\right) & e\text{ wave} \end{cases}. \tag{B3}$$

[1] M. Francoeur, M. Pinar Mengüç, R. Vaillon, and J. Quant, Spectrosc. Radiat. Transfer **110**, 2002 (2009).

[2] J. P. Mulet, K. Joulain, R. Carminati, and J.-J. Greffet, Microscale Therm. Eng. **6**, 209 (2002).

[3] S. Basu, Z. M. Zhang, and C. J. Fu, Int. J. Energ. Res. **33**, 1203 (2009).

[4] Z. H. Zheng and Y. M. Xuan, Int. J. Heat Mass Transfer **54**, 1101 (2011).

[5] X. L. Liu, L. P. Wang, and Z. M. Zhang, Nanosc. Microsc. Therm. **19**, 98 (2015).

[6] M. Francoeur, M. Pinar Mengüç, and R. Vaillon, J. Phys. D: Appl. Phys. **43**, 075501 (2010).

[7] S. A. Biehs and P. Benabdallah, Z. Naturforsch. A **72**, 0351 (2016).

[8] A. Narayanaswamy and G. Chen, Phys. Rev. B **77**, 075125 (2008).

[9] S. A. Biehs and J-J. Greffet, Phys. Rev. B **81**, 245414 (2010).

[10] S.-B. Wen, J. Heat Transfer **132**, 072704 (2010).

[11] B. Liu and S. Shen, Phys. Rev. B **87**, 115403 (2013).

[12] A. W. Rodriguez, O. Ilic, P. Bermel, I. Celanovic, J. D. Joannopoulos, M. Soljačić, and S. G. Johnson, Phys. Rev. Lett. **107**, 114302 (2011).

[13] A. W. Rodriguez, M. T. H. Reid, and S. G. Johnson, Phys. Rev. B **86**, 220302(R) (2012).

[14] S. Basu and M. Francoeur, Appl. Phys. Lett. **98**, 184301 (2011).

[15] S. Chen and G. D. Doolen, Annu. Rev. Fluid Mech. **30**, 329 (1998).

[16] L. S. Luo and S. S. Girimaji, Phys. Rev. E **67**, 036302 (2003).

[17] W. S. Jiaung, J. R. Ho, and C. P. Kuo, Numer. Heat Transfer, Part B **39**, 167 (2001).

[18] J. K. Wang, M. R. Wang, and Z. X. Li, Int. J. Therm. Sci. **46**, 228 (2007).

[19] J. R. Ho, C. P. Kuo, and W. S. Jiaung, Int. J. Heat Mass Transfer **46**, 55 (2003).

[20] Z. Guo and T. S. Zhao, Numer. Heat Transfer, Part B **47**, 157 (2005).

[21] C. K. Aidun and J. R. Clausen, Annu. Rev. Fluid Mech. **42**, 439 (2010).

[22] Y. Ma, S. K. Dong, and H. P. Tan, Phys. Rev. E **84**, 016704 (2011).

[23] X. P. Luo, C. H. Wang, Y. Zhang, H. L. Yi, and H. P. Tan, Phys. Rev. E **97**, 063302 (2018).

[24] C. Mchardy, T. Horneber, and C. Rauh, Opt. Express **24**, 16999 (2016).

[25] H. L. Yi, F. J. Yao, and H. P. Tan, Phys. Rev. E **94**, 023312 (2016).

[26] S. C. Mishra and H. K. Roy, J. Comput. Phys. **223**, 89 (2007).

[27] S. C. Mishra, T. B. P. Kumar, and B. Mondal, Numer. Heat Transfer, Part A **54**, 798 (2008).

[28] B. Mondal and S. C. Mishra, Numer. Heat Transfer, Part A **52**, 757 (2007).

[29] C. J. Fu and W. C. Tan, J. Quant. Spectrosc. Radiat. Transfer **110**, 1027 (2009).

[30] S. A. Biehs, F. S. S. Rosa, and P. Benabdallah, Appl. Phys. Lett. **98**, 243102 (2011).

[31] Y. Chen and Z. Zheng, Int. J. Heat Mass Transfer **125**, 589 (2018).

[32] A. Taflove and S. C. Hagness, *Computational Electrodynamics: The Finite-Difference Time-Domain Method*, 2nd ed. (Artech House, Norwood, MA, 1995).

[33] C. A. Balanis, *Advanced Engineering Electromagnetics*, 2nd ed. (Wiley, US, 2012).

[34] Cheng and K. David, *Field and Wave Electromagnetics*, 2nd ed. (Addison-Wesley Publishing Company, Inc., US, 1983).

[35] A. D. Boardman and T. Twardowski, Phys. Rev. A **39**, 2481 (1989).

[36] K. Joulain, J. P. Mulet, F. Marquier, R. Carminati, and J.-J. Greffet, Surf. Sci. Rep. **57**, 59 (2005).

[37] A. Najafi-Yazdi and L. Mongeau, Comput. Fluids **68**, 203 (2012).